European Journal of Pharmaceutical Sciences 138 (2019) 105017

Contents lists available at ScienceDirect

European Journal of Pharmaceutical Sciences

journal homepage: www.elsevier.com/locate/ejps

Biosensor-based kinetic and thermodynamic characterization of opioids interaction with human μ-opioid receptor

Hasan Babazada[a,*,1], Tural Alekberli[b], Parvana Hajieva[c], Elnur Farajov[d,*]

[a] Institute for Integrated Cell-Material Sciences, Kyoto University, Yoshidaushinomiya-cho, Sakyo-ku, Kyoto 606-8501, Japan
[b] Department of Anesthesiology and Critical Care Medicine, Hadassah Medical Center, The Hebrew University of Jerusalem, 91905 Jerusalem, Israel
[c] Cellular Adaptation Group, Institute for Pathobiochemistry, University Medical Center of the Johannes Gutenberg University, 55128 Mainz, Germany
[d] Department of Internal Medicine, Azerbaijan Medical University, AZ1000 Baku, Azerbaijan

ARTICLE INFO

Keywords:
Opioid
G-protein coupled receptor
Surface plasmon resonance
Kinetic selectivity
Transition state analysis
Activation
Thermodynamics

ABSTRACT

Development of opioid analgesics with minimal side effects requires substantial knowledge on structure–kinetic and –thermodynamic relationship of opioid-receptor interactions. Here, combined kinetics and thermodynamics of opioid agonist binding to human μ-opioid receptor (h-μOR) was investigated using real-time label-free surface plasmon resonance (SPR)–based method. The N-terminal end truncated and C-terminal 6His-tagged h-μOR was constructed and expressed in *E. coli*. Receptor was purified, detergent-solubilized and characterized by circular dichroism. The uniform immobilization of h-μOR on Ni-NTA chips was achieved using hybrid capture-coupling approach followed by reconstitution in lipid bilayer. Thermodynamic equilibrium affinities of opioids were in narrow nanomolar range and in near quantitative agreement with their K_i values. However, they did not correlate with their *in vitro* EC_{50} values, indicating that they might not have thermodynamic selectivity. Contrary, on and off rates exhibited much larger dispersion and well correlated with EC_{50} values, indicating that opioids might exhibit kinetic-selectivity towards their target. Temperature-dependent SPR assays provided access to rate and equilibrium thermodynamic data, which demonstrated binding of morphine and naloxone to μOR was exothermic and essentially enthalpy driven. This work suggests that kinetic-based structure-activity of opioids in drug design and incorporation into the pharmacokinetics-pharmacodynamics predictions may have more value than thermodynamic equilibrium constants alone.

1. Introduction

The μ-opioid receptor (μOR), a member of the G protein-coupled receptor (GPCR) superfamily, is a molecular target for the treatment of pain and related psychiatric disorders, and critically involved in modulating social behavior (Pellissier et al., 2017). Although opioids targeting μOR are the most used analgesics in clinical practice, minimizing side effects while improving clinical efficacy has been impeded by difficulties in methodologies to investigate biophysical properties of ligand-receptor interactions. In clinical trials, pain is controlled by gradually titrating opioids to determine optimal dose necessary for balance between adequate pain relief and side effects (Katz, 2005; Petrone et al., 1999). It appears that even though efficacies of the drug candidates are well characterized, lack of clear understanding about biophysical properties such as kinetics and thermodynamics of ligand-target interactions prevents to discriminate analgesic effect from side effects in early times and results in increased failure rate of clinical trials. Moreover, some full agonists of μOR like morphine and methadone exhibit very similar affinities but dramatically different effective analgesic scores as well as severity and risk factors for adverse reactions (Mercadante et al., 1998). This argues that these compounds may have no thermodynamic selectivity but still have kinetic selectivity (de Witte et al., 2016) to the same target if their association and dissociation rates are different. Although, equilibrium values such as IC_{50}, K_D or K_i quantified at constant concentrations provide the affinity-based potency and binding information; they give no insight in to the kinetic-based potency. This is especially important in determining the role of dissociation rate and residence time in drug potency (Copeland et al., 2006; Swinney, 2006). Therefore, binding kinetic and thermodynamic characteristics of opioids should be fully utilized and incorporated into the pharmacokinetic-pharmacodynamics (PKPD) models to predict the drug activity. Such characterization would be detrimental in revealing

* Corresponding authors.
E-mail addresses: hasan.babazada@uphs.upenn.edu (H. Babazada), dr.elnur.farajov@gmail.com (E. Farajov).
[1] Present address: Department of Radiology, Perelman School of Medicine, University of Pennsylvania, 3620 Hamilton Walk, Philadelphia, 19104 PA, USA.

https://doi.org/10.1016/j.ejps.2019.105017
Received 27 May 2019; Received in revised form 11 July 2019; Accepted 25 July 2019
Available online 26 July 2019

trade-off between analgesic and side effects, which could occur even at sub-optimal doses (Jamison et al., 1998).

Surface plasmon resonance (SPR) is widely applied to study biomolecular interactions (Rich and Myszka, 2000). Despite the intrinsic prerequisites of SPR, such as immobilization of one binding partner while retaining its structural and functional activity, SPR remains a powerful analytical tool as it offers sensitive (picomolar range), label-free and real-time measurements of binding kinetics and thermodynamics. Although, GPCRs are conveniently expressed and scaled up in *E. coli* with proper post-translational modifications (Grisshammer et al., 1993; Ren et al., 2009; Stanasila et al., 1999; Tucker and Grisshammer, 1996), their immobilization onto the SPR sensor chips in a function-retaining manner and in sufficient density is challenging.

Here, to analyze complete kinetic and thermodynamic characteristics of opioid–μOR interactions, we expressed and detergent-purified N-terminal end truncated and C-terminal his-tagged human μOR (h-μOR), which was then assembled onto the SPR chip by capture-coupling and reconstitution. This method produces uniformly oriented native h-μOR in lipid bilayer. Reconstitution in lipid layers mimics biological membranes and is critically involved in receptor functionality including facilitating structural reorientation in agonistic/antagonistic activation as well as G protein binding. This approach allowed directly obtaining and analyzing high-quality kinetic, affinity and thermodynamic data and temperature-dependent kinetics of opioid-μOR interaction in a real-time fashion. Importantly, free energy difference between ground and transition states for binding of morphine to h-μOR, which controls the association and dissociation of the compound was investigated. Furthermore, our data reveal quantitative agreement between kinetic/affinity values and reported *in vitro* K_i and EC_{50} values, obtained using μOR agonist-stimulated [^{35}S]guanosine-5′-O-(3-thiotriphosphate) ([^{35}S]GTPγS) binding assays.

2. Materials and methods

2.1. Expression and purification of recombinant human μ opioid receptor

The pET-28b + vector that encodes C-terminal His-tagged and N-terminal end truncated (Δaa 1-65) variant of human μOR in between the *BamHI* and *XbaI* restriction sites under the control of T7 transcription was transformed and expressed in BL21 (DE3) cells. The receptor was then purified using nickel-resin affinity chromatography as described previously with some modifications (Ma et al., 2013). Briefly, harvested cells were lysed in buffer containing 1 M urea in 50 mM Tris-HCl, pH 8.0, 10% Glycerol, 0.1% Triton X-100, lysozyme (1 μg per OD of cells), 5 mM $MgCl_2$, 2 mM 2-Mercaptoethanol, 1 mM EDTA and 100 U of benzonase. The cell lysate was centrifuged at 10000*g* for 20 min to collect inclusion bodies. The supernatant was further ultra-centrifuged at 120000*g* for 90 min to harvest membrane fractions. The membrane pellets were resuspended in 20 mM Tris–HCl, 300 mM NaCl, 10% Glycerol, pH 8 and 1% Fos-Choline-12 and gently agitated for 2 h at 4 °C. Supernatant containing solubilized receptor was separated by centrifugation at 12000*g* for 20 min and subsequently applied to nickel affinity column. Captured receptor was washed with buffer containing 20 mM Tris–HCl, 300 mM NaCl, 10% Glycerol, pH 8 and 0.1% Fos-Choline-12, and eluted in fractions with buffer containing 20 mM Tris–HCl, 300 mM NaCl, 10% Glycerol, pH 8, 0.1% Fos-Choline-12 and 300 mM imidazole. Solution of h-μOR was dialyzed against 20 mM sodium phosphate, 150 mM NaCl, pH 8 and 0.1% Fos-Choline-12.

2.2. Circular dichroism measurements

Circular dichroism (CD) spectra were collected using AVIV Model 410 Circular Dichroism spectrophotometer (Aviv Biomedical Inc., USA) using h-μOR at concentration of 0.2 mg/mL in 20 mM sodium phosphate, 150 mM NaCl, pH 8 and 0.1% Fos-Choline-12. Spectra were recorded from 260 to 185 nm with a step size and bandwidth of 1 nm. Thermal ramping were performed from 10 °C to 90 °C with the rate of 1 °C/min, 0.2 °C tolerance and 0.5 °C step size. Results were recorded in millidegrees and converted to mean residue ellipticity, θ, deg.·cm^2·dmol^{-1}. Data were collected using CDS Program (Aviv Biomedical Inc., USA). Spectra were averaged from five scans and smoothed using a Savitzky-Golay algorithm (Savitzky and Golay, 1964). All CD data were corrected by subtracting the spectrum of buffer alone. Spectra were deconvoluted using BeStSel program (Micsonai et al., 2015).

2.3. Surface plasmon resonance

SPR experiments were carried out using a ProteOn™ XPR36 Protein Interaction Array System (Bio-Rad Laboratories, Inc., Hercules, CA). Hybrid capture-coupling strategy was utilized to immobilize detergent-solubilized h-μOR in the presence and absence of a reconstituted bilayer (Rich et al., 2011). The sensor chip tris-Nitrilotriacetic Acids (NTA) surface was first activated using 1-Ethyl-3-(3-dimethylaminopropyl) carbodiimide (EDC) and N-Hydroxysuccinimide (NHS) reagents, according to the standard procedure for amine coupling. The surface then Ni2 + -charged according the manufacturer's protocol. For direct capture-coupling of C-His-tagged h-μOR (in running buffer of 10 mM HEPES, pH 7.4, and 0.15 M NaCl supplemented with 0.1% Fos-Choline-12) detergent-purified receptor was diluted to 10 μg/mL in running buffer and injected at 5 μL/min until the immobilization levels reached 2000–3000 resonance units (RU). In a separate channel immediately after the immobilization of detergent-solubilized h-μOR, a 1-palmitoyl-2-oleoyl-sn-glycero-3-phosphocholine (POPS) lipid bilayer was reconstituted by injecting a mixture of 3 mM POPC and 3 mM Fos-Choline-12 for 30 min. The remaining surface-active groups were blocked with 1 M ethanolamine hydrochloride, pH 8.5. A reference surfaces were also generated where the channel was activated and blocked with or without subsequent reconstitution of a lipid bilayer. All sensorgrams corresponding to the directly capture-coupled or lipid-reconstituted receptor were double referenced (signals from the reference channels without and with lipid bilayers are subtracted from the acquired signal in the h-μOR channels and corrected with a blank buffer injection).

2.4. Kinetic characterization of opioid agonists

For kinetic constants and K_D measurements, at least five gradient concentrations of morphine sulfate pentahydrate, fentanyl citrate, buprenorphine hydrochloride and methadone hydrochloride (Sigma Aldrich, St. Louis, MO, USA) from 0.625 to 20 nM were prepared in running buffer and flowed at 60 μL/min over the immobilized surface for 2 min at 25 °C. Double referenced data were analyzed using non-linear least squares analysis method as described previously (O'Shannessy et al., 1993). OriginPro 2015 (OriginLab Corporation, MA) was used for routine curve fitting of integrated rate equations

$$R_t = Re^{-k_{off}t} \quad (1)$$

and

$$R = [C]k_{on}R_{max}[1 - e^{-(([C]k_{on}+k_{off})t)}]/[[C]k_{on} + k_{off}] \quad (2)$$

for dissociation and association phases respectively, where k_{on} and k_{off} are rate constants, R_{max} is maximal response, [C] is the concentration of analytes.

2.5. Determination of thermodynamic parameters of equilibrium

Temperature-dependent studies of morphine and h-μOR interactions were conducted at 15, 20, 25, 30 and 35 °C. At each temperature point the instrument was equilibrated for at least 30 min before the measurements. Two-fold serial dilutions of morphine in running buffer were prepared and injected for 2 min over the immobilized detergent-solubilized h-μOR at a flow rate of 60 μL/min. The derived affinity constant

K_A ($K_A = k_{on}/k_{off}$ or $K_A = 1/K_D$) at various temperatures from 15 to 35 °C were fitted with the non-linear integrated form of van't Hoff equation, where the enthalpy is not temperature-independent ($\Delta C_p \neq 0$):

$$\ln K_A = \frac{\Delta H^\circ(T_o) - T_o \Delta C_p}{R}\left(\frac{1}{T_o} - \frac{1}{T}\right) + \frac{\Delta C_p}{R}\ln\left(\frac{T}{T_o}\right) + \ln K_o \quad (3)$$

where, K_o is the equilibrium association constant at reference temperature $T_o = 298.15$ K; ΔH° is standard enthalpy at T_o; ΔC_p is heat capacity at constant pressure; R is the universal gas constant (8.314 J mol^{-1} K^{-1}). For linear van't Hoff plots, the standard enthalpy and entropy were obtained by fitting the data to equation:

$$\ln K_A = \frac{-\Delta H^\circ}{R}\frac{1}{T} + \frac{\Delta S^\circ}{R} \quad (4)$$

2.6. Determination of transition state formation

Kinetic data can be analyzed by use of the Eyring's theory. For linear Eyring plots of $\ln(k_{off}h/k_BT)$ *vs* $1/T$, the enthalpy ($\Delta H^{\circ\ddagger}$) and entropy ($\Delta S^{\circ\ddagger}$) of the activation were obtained by fitting the data with equation:

$$\ln\left(\frac{k_{off}h}{k_BT}\right) = \frac{-\Delta H^{\circ\ddagger}}{R}\frac{1}{T} + \frac{\Delta S^{\circ\ddagger}}{R} \quad (5)$$

where, k_{off} is the off rate constant; h is Planck's constant (6.626×10^{-34} J s); and k_B is Boltzmann's constant (1.381×10^{-23} J K^{-1}). For the nonlinear Eyring plots of the on rate k_{on}, data were fitted with the nonlinear Eyring equation:

$$\ln\left(\frac{k_{on}h}{k_BT}\right) = \frac{-\Delta H^{\circ\ddagger}}{R}\frac{1}{T} + \frac{\Delta S^{\circ\ddagger}}{R} + \frac{\Delta C_p(T^\circ - T)}{R}\frac{1}{T} + \frac{\Delta C_p}{R}\ln\left(\frac{T}{T^\circ}\right) \quad (6)$$

Python scripts using *curve_fit* package from *scipy.optimize* module were developed for routine fitting of thermodynamic and kinetic data.

3. Results and discussion

3.1. Expression and characterization of h-μOR

The h-μOR protein expressed well in *E. coli*. Purity up to ~90% was achieved using nickel-ion affinity chromatography. Other contaminants were removed by dialyzing the protein against a solution of 20 mM sodium phosphate buffer (pH = 8.0), 150 mM NaCl containing 0.1% Fos-Choline-12. A single major band with the estimated mass of purified h-μOR (~40 kDa) was observed on Western blot (not shown). The α-helical content was estimated to be 48.1% as obtained from deconvolution of its CD spectrum at 25 °C (Fig. 1a). The folding of the receptor was in agreement with reported values for N-terminal truncated human h-μOR (47 ± 3%) (Muller et al., 2010). The temperature dependence of the CD signal at 222 nm revealed that h-μOR lost ellipticity with increasing temperature (Fig. 1b), exhibiting a melting temperature of $T_m = 70$ °C as obtained from the maximum of the first derivative dθ/dT at 222 nm (Fig. 1c).

3.2. Kinetics of opioids binding to the h-μOR

To analyze the affinity and kinetics of opioids with h-μOR, detergent-solubilized receptor was immobilized onto the SPR sensor chip using hybrid capture-coupling strategy, in which the nickel-charged NTA surface is activated with an EDC/NHS mixture prior to injection of the receptor. With this strategy the receptor is first preconcentrated *via* the His-tag for subsequent covalent immobilization *via* the activated carboxyl groups as previously described for His-tagged StaR $A_{2A}R$ and β^1AR proteins (Rich et al., 2011). This allows capturing receptor at C-terminal, which produces uniformly oriented stable protein layers on the sensor surface with N-terminal facing the solvent. Such orientation of receptor molecules allows controlling the access to binding pocket on the receptor for quantitative studies of opioid interaction. The immobilized receptor was immediately on-surface reconstituted in lipid bilayer (Karlsson and Löfås, 2002; Stenlund et al., 2003). The schematic of immobilization strategy is shown in Fig. 2a. We analyzed affinity and kinetics of five opioids with different physicochemical and pharmacological properties. In order to avoid mass transfer limitations and non-Langmuirian kinetics due to steric hindrance between immobilized receptors, an R_{max} of ~2000 RU (1 RU = 1 pg of protein per mm^2) was used for the binding studies, which was sufficient for quantification of all analytes. More than 80% of immobilized h-μOR preserved functionality, as determined by the ratio of measured SPR responses in the presence and absence of opioids. Opioids were injected over the functionalized surface for 2 min at gradient concentrations between 0.625 and 20 nM. The SPR sensorgrams were well fit by a 1:1 binding model. Morphine, methadone, buprenorphine, fentanyl, and naloxone bound to h-μOR with K_D of 4.3, 3.4 nM, 1.3 nM, 1.7 nM, and 3.4 nM respectively (Fig. 2b, Table 1). These affinities were compared with literature equilibrium inhibition constant values (K_i) obtained from *in vitro* competition binding experiments using [3H]DAMGO (Bento et al., 2014). There is a good correlation (Pearson's $r = 0.93$) between the SPR-derived K_D and these K_i values (Fig. 3a); indeed, these equilibrium constants are in near quantitative agreement ($P = 0.02$ by the two-tailed Student's *t*-test).

Although only the small differences in the thermodynamic equilibrium affinities among these tested opioids were observed, the kinetic rates of association and dissociation in different agonists could be resolved, which indicated kinetic specificity in formation of opioid–h-μOR complexes.

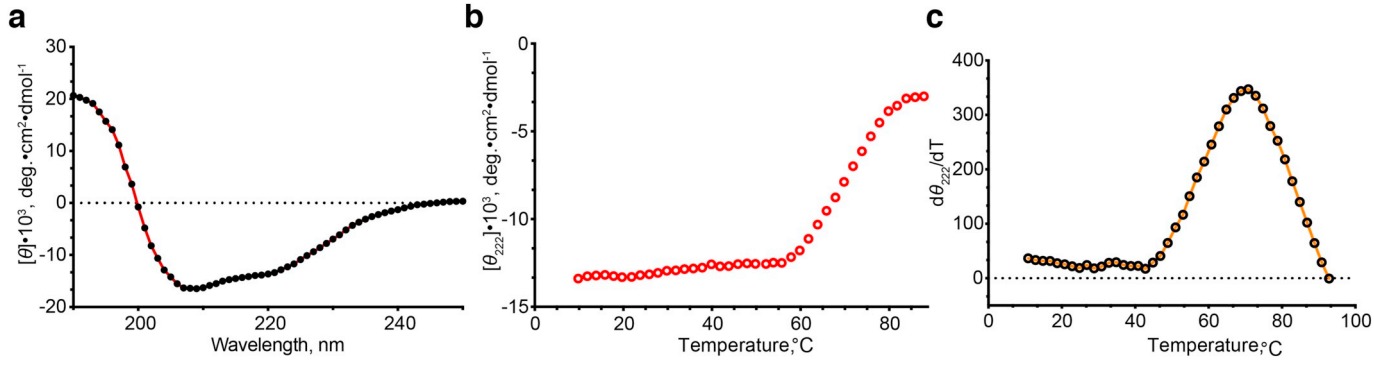

Fig. 1. Secondary structural analysis of detergent-purified h-μOR.
(a) CD spectrum of h-μOR (0.2 mg/mL) solubilized in 20 mM sodium phosphate, 150 mM NaCl, pH 8 and 0.1% Fos-Choline-12 in a 0.1 cm cuvette. Average of five measurements recorded at 25 °C and was deconvoluted to determine the secondary structure content. (b) The mean residue ellipticity at 222 nm collected as a function of temperature. (c) Estimation of the melting temperature from the maximum of the first derivative dθ/dT at 222 nm.

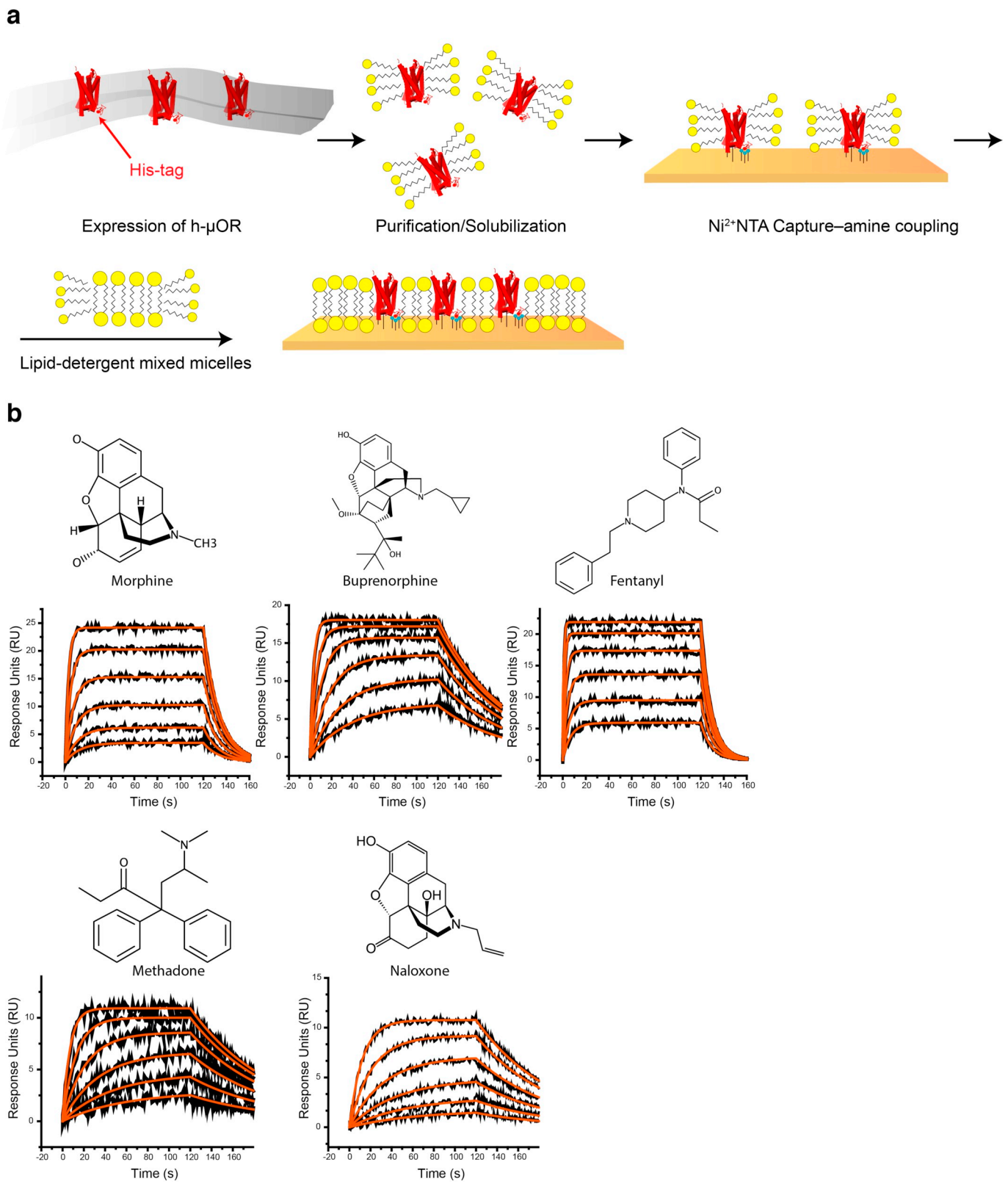

Fig. 2. Surface plasmon resonance measurements of opioids binding to h-μOR. (a) Schematic illustration of receptor immobilization strategy. Capture of a detergent-solubilized h-μOR *via* C-terminal His-tag onto a Ni^{2+} NTA chip followed by amine coupling and injection of lipid–detergent mixed micelles and formation of a lipid bilayer. (b) Sensorgrams of the binding of opioid ligands that were injected at concentrations ranging from 0.625 to 20 nM over the captured h-μOR surface at 25 °C. Double referenced data were fit using the nonlinear least squares method. Data are representative of three independent measurements.

Table 1
Kinetic and affinity constants determined for opioid–h-μOR interactions using SPR.

Opioid compound	k_{on} $M^{-1}{\cdot}s^{-1}$	k_{off} s^{-1}	K_D nM	K_i nM	$t_{1/2}$ s
Morphine	3.6×10^7 (± 2.3)	7.1×10^{-2} (± 0.4)	4.3 (± 1.9)	3.5 (± 1.9)	9.8 (± 0.6)
Fentanyl	5.3×10^7 (± 0.6)	8.7×10^{-2} (± 1.1)	1.7 (± 0.3)	1.6 (± 0.4)	8.2 (± 1.0)
Methadone	6.9×10^6 (± 1.7)	1.9×10^{-2} (± 0.3)	3.4 (± 1.4)	2.6(± 2.5)	38.1 (± 7.1)
Buprenorphine	1.0×10^7 (± 0.3)	1.3×10^{-2} (± 0.2)	1.3 (± 0.2)	1.8 (± 0.5)	58.0(± 12.2)
Naloxone	4.4×10^6 (± 1.4)	1.4×10^{-2} (± 0.1)	3.4 (± 0.9)	3.63 (± 0.4)	48.4 (± 1.9)

Dissociation half-life time calculated from $t_{1/2} = \ln(2)/k_{off}$.
Data represent the mean ± standard error of three independent experiments using different sensor chips. K_i values for agonists were obtained from database that reports μOR agonist-stimulated [^{35}S]GTPγS binding assays. K_i values for naloxone were obtained using CHO cell membranes stably expressing μ receptors with [^{3}H] diprenorphine as reference ligand (Schlechtingen et al., 2003).

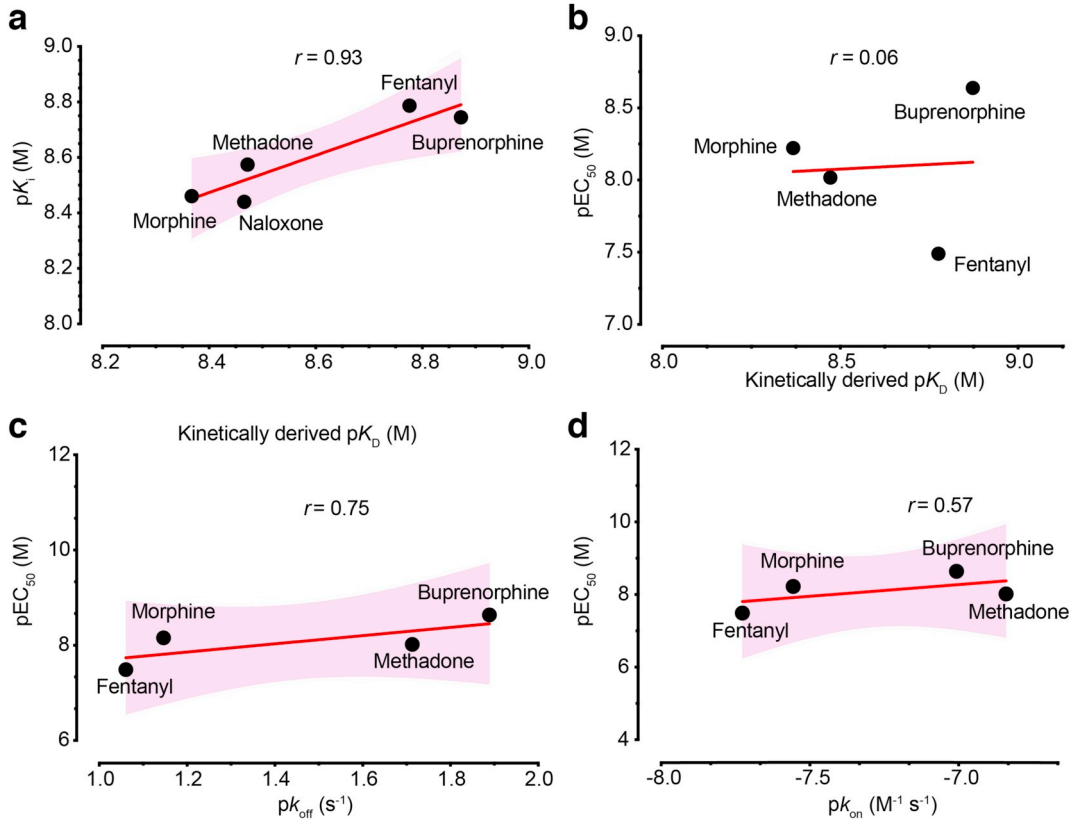

Fig. 3. Affinity and kinetic constants of opioid–h-μOR relative to their EC_{50} values. (a) Correlation between SPR-derived $pK_D = -log_{10}$ (K_D/M) values and *in vitro* $pK_i = -log_{10}$ (K_i/M) values (M = mol/L). (b) Correlation between pK_D and pEC_{50} values. (c) Correlation between pEC_{50} and dissociation rate constant; $pk_{off} = -log_{10}$ (k_{off}/s^{-1}). (d) Correlation between pEC_{50} and association rate constant; $pk_{on} = -log_{10}$ ($k_{on}/M^{-1}\,s^{-1}$). The shadowed area identifies the 95% confidence interval. Red line in each plot is a linear least squares fit to the data. (For interpretation of the references to colour in this figure legend, the reader is referred to the web version of this article.)

Relatively slow association and dissociation was observed for buprenorphine ($k_{on} = 1.0 \times 10^7\,M^{-1}{\cdot}s^{-1}$, $k_{off} = 1.3 \times 10^{-2}\,s^{-1}$), methadone ($k_{on} = 6.9 \times 10^6\,M^{-1}{\cdot}s^{-1}$, $k_{off} = 1.9 \times 10^{-2}\,s^{-1}$) and naloxone ($k_{on} = 4.4 \times 10^6\,M^{-1}{\cdot}s^{-1}$, $k_{off} = 1.4 \times 10^{-2}\,s^{-1}$), while fentanyl ($k_{on} = 5.3 \times 10^7\,M^{-1}{\cdot}s^{-1}$, $k_{off} = 8.7 \times 10^{-2}\,s^{-1}$) and morphine ($k_{on} = 3.6 \times 10^7\,M^{-1}{\cdot}s^{-1}$, $k_{off} = 7.1 \times 10^{-2}\,s^{-1}$) exhibited more rapid association and dissociation rates. Elevated dissociation half-life values of buprenorphine ($t_{1/2} = 58$ s) and methadone ($t_{1/2} = 38$ s) as compared to the other opioid agonists (Table 1) may suggest that the onset and decline of the pharmacological effect is predominantly determined by the presence and retention of these compounds in the effect site of the receptor. Consistently with their residence times, both buprenorphine and methadone are shown to have long half lives *in vivo* (Grissinger, 2011; Huestis et al., 2013; Krantz et al., 2005). Half-life of naloxone was shorter than that of buprenorphine. Previous studies of mechanism-based PKPD modelling of the reversal of buprenorphine-induced respiratory depression by naloxone revealed a competitive interaction between buprenorphine and naloxone at μOR. It has been shown that slow receptor association/dissociation kinetics of buprenorphine *in vivo*, the short half-life of naloxone elimination from the brain complicate rapid and complete reversal of buprenorphine-induced respiratory depression (Yassen et al., 2007). Although we did not observe slower association rate for buprenorphine as compared to naloxone, our data supports that faster dissociation *i.e.* shorter half-life of naloxone on the opioid receptors functioning in respiratory depression requires naloxone to be administered as a continuous infusion for reversal of buprenorphine-induced respiratory depression. Fentanyl exhibits a shorter residence half-life of $t_{1/2} = 8$ s, and therefore could be more sensitive to the local receptor concentration such as number of receptors per cell. It could suggest the effect of ligands like fentanyl could arise from the ability to rapidly come on/off and excite multiple receptors, although further studies are needed to

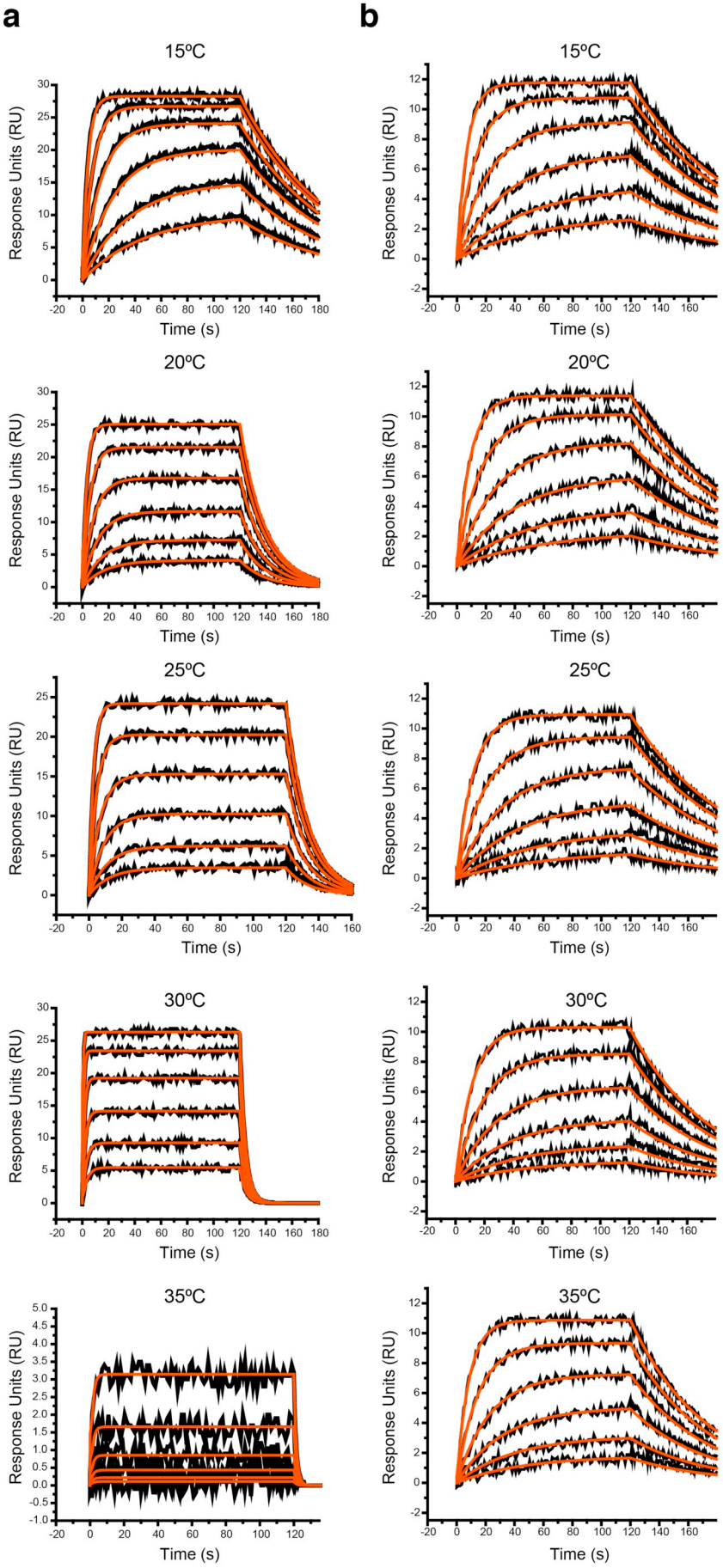

(caption on next page)

Fig. 4. Temperature dependence of the biosensor binding response for morphine– and naloxone–h-μOR interactions. The black lines represent the biosensor responses obtained for a concentration series of (a) morphine or (b) naloxone (0.625 to 20 nM) injected in triplicate across a lipid reconstituted h-μOR surface (~2000 RU) at indicated temperatures. The orange lines represent global fits to a simple bimolecular interaction model.

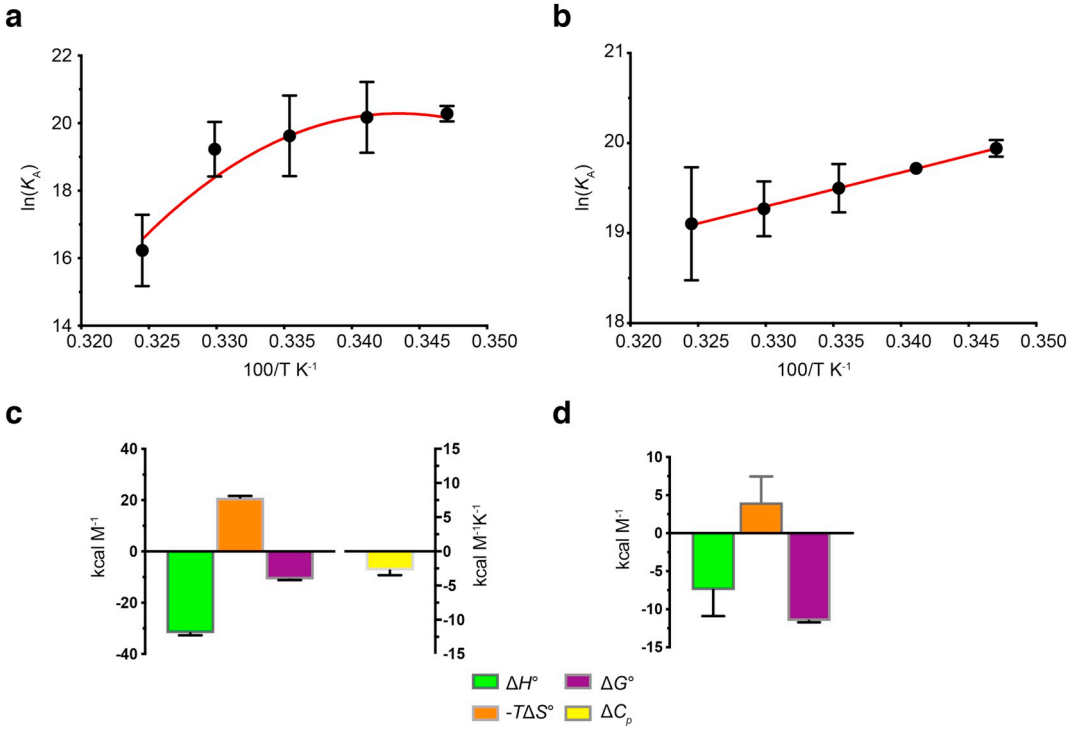

Fig. 5. Thermodynamic equilibrium analysis of morphine– and naloxone–h-μOR interactions. The van't Hoff plot for binding of morphine (a) and naloxone (b) to h-μOR determined from temperature-dependent biosensor analysis. Least squares analysis was used to fit data with nonlinear (a) and linear (b) van't Hoff equation. Thermodynamic profile of morphine (c) and naloxone (d) binding to h-μOR derived from biosensor analysis at 298 K. The error bars indicate ± SD in the experimental affinity data. Data and uncertainties were obtained from three independent measurements.

confirm this. There was no appreciable difference observed in kinetics of opioids in non-reconstituted surface, where detergent-solubilized receptor was directly capture-coupled onto the chip. However, assembling the receptor within lipid bilayer is advantageous for functional retention of the receptor and mimicking the native cell membrane environment. It is very clear that membrane associations play a critical role in retention and functionality of G proteins (Jastrzebska et al., 2011; Vögler et al., 2008; Zhang et al., 2004). That said, it is possible to place the 6-His tag to N-terminal, thereby reorient and uniformly immobilize μOR exposing C-terminal segment outwards following the reconstitution in lipid bilayer for direct detection of G-protein opioid agonist-induced activation as shown previously for rhodopsin (Bieri et al., 1999).

3.3. Relationship between agonist efficacy and binding kinetic rate constants

Because the kinetic rate constants varied across the tested opioids, we analyzed whether kinetic rate constants and affinities could be correlated with potency data. An opioid-induced [^{35}S]GTPγS binding assay has been used to determine the pharmacological potency of opioids (Strange, 2010), and in this study we used the EC_{50} values to analyze the correlation with kinetic and affinity parameters of opioid-μOR binding. The average [^{35}S]GTPγS binding EC_{50} values for morphine (6 nM ± 2 nM) (Nikolaev et al., 2007), fentanyl (32.4 ± 2.8 nM) (Bento et al., 2014), methadone (9.6 ± 1.5 nM) (Blake et al., 1997) and buprenorphine (2.3 ± 1.7 nM) (Husbands et al., 1999) were obtained from ChEMBL database (Bento et al., 2014) and served to define the potencies of the opioids. The pK_D values of opioid agonists did not correlate with pEC_{50} (Pearson's $r = 0.06$) (Fig. 3b). In contrast, dissociation rate constant, pk_{off} correlated well with pEC_{50} (Pearson's $r = 0.75$) (Fig. 3c). Association rate constant, pk_{on} moderately correlated with pEC_{50} (Pearson's $r = 0.57$) (Fig. 3d). Correlation analyses suggest that kinetic rate constants can be more valuable parameters than affinities alone to define the *in vivo* efficacy of opioids at μOR. It suggests that the impact of kinetic selectivity of opioids should be prioritized in defining their therapeutic efficacies for the μOR. The data are consistent with decreasing EC_{50} (higher potency) as the dynamic rates associated with ligand-receptor exchange (k_{off} and k_{on}) decrease. Data suggest that dynamics may be more relevant and correlate better with activity than affinity, but more work is needed to show that conclusively. Although, Pearson's r values are far from zero, more opioids need to be analyzed to decide whether the linear relationship in the sample data is strong enough to use to model the relationship in the population.

When considering the relationship of biophysical properties of opioids and their efficacies in drug-target interactions, it is worth noting that some opioids undergo multiphase metabolism to either inactive, equally potent, or compounds with weaker or higher affinities and analgesic activities. For example, oxymorphone has a greater binding affinity to μOR than parent drug oxycodone, while noroxycodone and the reduced metabolites α- and β-oxycodol have weaker binding affinities to μOR compared to oxycodone (Lalovic et al., 2006). Moreover, morphine has a slightly higher affinity for the μOR than its metabolite Morphine-O6-glucuronide (M6G), whereas M6G shows higher efficacy at the μOR (Kilpatrick and Smith, 2005). Consistently with our data it implies that affinities at molecular level may not necessarily correlate with the potencies of opioids. Evidently, more studies focused on individual drugs and their metabolites will be needed to

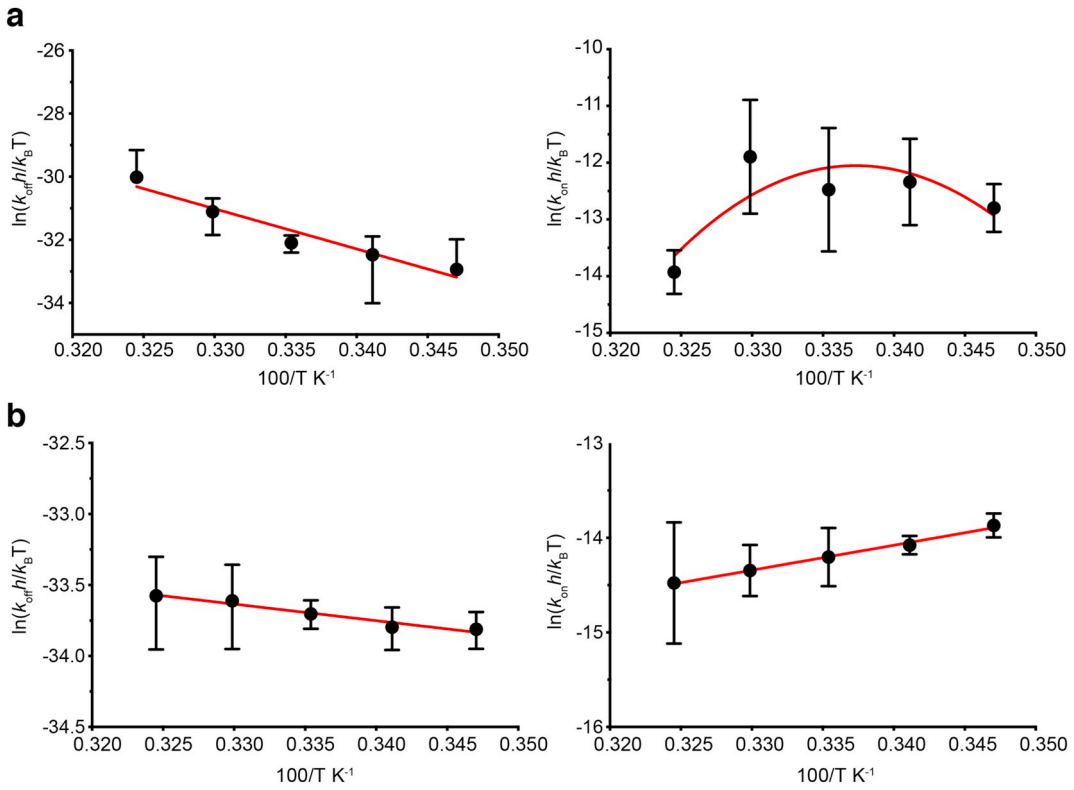

Fig. 6. Transition state analysis of morphine– and naloxone–h-μOR interactions. Eyring plots for morphine (a) and naloxone (b) interactions with h-μOR in terms of k_{off} and k_{on}, determined from biosensor analyses. Least squares analysis was used to fit the data to either linear or nonlinear forms of Eyring equations. The error bars indicate ± SD in the experimental kinetics data. Data and uncertainties were obtained from three independent measurements.

demonstrate that convincingly.

3.4. Thermodynamic equilibrium analysis of morphine and naloxone binding to the h-μOR

Thermodynamics of opioid–μOR interactions can give insight into the nature of binding and thereby assist rational drug design. To investigate the surface-based thermodynamic parameters for the morphine– (Fig. 4a) and naloxone–h-μOR interactions (Fig. 4b), binding data were collected at 15, 20, 25, 30 and 35 °C on the biosensor. It should be indicated that there could be potential structural fluctuations associated with the protein given the variation in temperature. However, CD results suggest no cooperative unfolding at tested range.

The sensorgrams were well fit to a 1:1 binding model to obtain temperature-depended affinity and kinetic rate constants. SPR analysis showed that affinities of both morphine and naloxone for h-μOR decreased as temperature was increased. The equilibrium dissociation constant for binding, K_D, of morphine increased from 1.6 nM to 118 nM over this temperature range. The changes of K_D values of naloxone were not vivid as in morphine and increased about 3-fold from 2.2 nM to 5.8 nM. Temperature-dependent equilibrium constants of morphine–h-μOR interaction were used to determine the thermodynamic parameters from a van't Hoff plot of $\ln(K_A/M)$ *vs* $1/T$. As shown in Fig. 5a, the van't Hoff plot has a convex shape, suggesting that the heat capacity is not constant but that the binding is predominantly enthalpy driven at 25 °C. Fitting the data to the nonlinear van't Hoff equation yielded the following, where the standard values of ΔH° and ΔS° are those at $T = 298.15$ K: $\Delta H^\circ = -32 \pm 0.7$ kcal mol^{-1}, $-T\Delta S^\circ = 21 \pm 0.6$ kcal mol^{-1}, and $\Delta C_p = -2.8 \pm 0.7$ kcal mol^{-1} K^{-1}. $\Delta G^\circ = -11 \pm 0.2$ kcal mol^{-1} could be determined from $\Delta G^\circ = -RT \ln(K_A/M)$ using equilibrium association constant at 298.15 K. The changes in the Gibbs free energy of binding of morphine were consistent with ΔG° values obtained in other thermodynamic studies (Fábián et al., 1996; Li et al., 1998). Values of K_A of naloxone obtained at each temperature were fitted using linear regression (Fig. 5b), which yielded $\Delta H^\circ = -7.5 \pm 3.4$ kcal mol^{-1} and $-T\Delta S^\circ = 4.05 \pm 0.17$ kcal mol^{-1} (reference T = 298.15 K). $\Delta G^\circ = -11.5 \pm 0.17$ kcal mol^{-1} for naloxone–h-μOR interaction was determined from $\Delta G^\circ = -RT \ln(K_A/M)$ at 298.15 K. The negative sign of ΔH° in both morphine (Fig. 5c) and naloxone indicated that nature of their binding was exothermic (Fig. 5d). The magnitude of the change in free energy found in this study is in good agreement with values reported for a variety of ligand-GPCR interactions regardless of methodology used.

3.5. Transition state analysis

The values of thermodynamic equilibrium provide limited to no information on the rate of complex formation. The temperature dependence of on and off rate constants allows analysis of the thermodynamics of the transition state, using Eyring plots (Sharma and First, 2009). Moreover, transition state analysis can provide insights on how interactions with similar affinities can have different kinetics. Intrinsic barrier crossing rates are difficult to determine, and herein we choose the simplest form for the exponential prefactor (k_BT/h); the reported values of $\Delta G^\ddagger$ and $-T\Delta S^\ddagger$ are necessarily dependent on this choice. It can be seen from the plot of $\ln(kh/k_BT)$ *vs* $1/T$ that the dissociation rate constant is linear in 1/T and slightly dependent on the temperature, indicating a positive activation enthalpy for both morphine (Fig. 6a) and naloxone (Fig. 6b) with $\Delta H^\ddagger = 21 \pm 0.6$ kcal mol^{-1} and $\Delta H^\ddagger = 2.3 \pm 0.6$ kcal mol^{-1}, respectively, for the dissociation process. Linear regression analysis of dissociation data of morphine yielded $-T\Delta S^\ddagger = 2.3 \pm 0.8$ kcal mol^{-1} and $\Delta G^\ddagger = 18 \pm 0.2$ kcal mol^{-1}, whereas for naloxone $-T\Delta S^\ddagger = 17.7 \pm 0.6$ kcal mol^{-1} and $\Delta G^\ddagger = 19.9 \pm 0.01$ kcal mol^{-1}. However, in contrast to naloxone, association rate data of morphine was nonlinear at higher temperatures, giving the Eyring plot of $\ln(k_{on}h/k_BT)$ *vs* $1/T$ a convex structure

(Fig. 6a), which indicates large heat capacity associated with binding. Fitting the association data of morphine to the nonlinear Eyring equation yielded the activation parameters for binding $\Delta H^{\ddagger} = -11 \pm 0.2\,\mathrm{kcal\,mol^{-1}}$, $-T\Delta S^{\ddagger} = 17 \pm 0.1\,\mathrm{kcal\,mol^{-1}}$, $\Delta C_p^{\ddagger} = 4.4 \pm 2.2\,\mathrm{kcal\,mol^{-1}\,K^{-1}}$ and $\Delta G^{\ddagger} = 7 \pm 0.8\,\mathrm{kcal\,mol^{-1}}$. Eyring analysis using linear regression of temperature-dependent association constants of naloxone resulted activation parameters of $\Delta H^{\ddagger} = -5.3 \pm 4.4\,\mathrm{kcal\,mol^{-1}}$, $-T\Delta S^{\ddagger} = 13.7 \pm 4.4\,\mathrm{kcal\,mol^{-1}}$, and $\Delta G^{\ddagger} = 8.9 \pm 0.17\,\mathrm{kcal\,mol^{-1}}$. Establishment of transition state for these interactions was associated with negative enthalpy contribution to free energy. This suggests a net increase of bonding energy on formation of active intermediate. Activation parameters of binding and unbinding for morphine and naloxone were inline with those obtained for GPCRs and small molecule interactions using SPR (Deganutti et al., 2017).

4. Conclusion

The N-terminal truncated and C-terminal 6-His tagged detergent-purified human μOR was hybrid capture-coupled onto the NTA sensor chip, thereby uniformly orienting ligand-binding pocket outwards. Surface was then reconstituted in lipid bilayer using lipid/detergent mixed micelles to mimic the native membrane environment. Opioid agonists preferentially bound to μOR with comparable K_D values in a narrow nanomolar range. Thermodynamic equilibrium affinities were in near quantitative agreement with previously reported values of K_i for the four ligands studied validating this approach. However, equilibrium affinities were not correlated with EC_{50} values indicating that opioids might not exhibit thermodynamic selectivity. On the other hand, on and off rates, exhibited a much larger dispersion in their values, and well correlated with EC_{50} values, suggesting that opioid agonists demonstrate kinetic selectivity towards their target. These results suggest that consideration of kinetic-based structure activity of opioids *i.e.* on and off rate constants in drug design and incorporation into PKPD predictions could have more value than thermodynamic equilibrium affinity constants alone. Thus, the identification of μOR target compounds based on their kinetic effects is essential.

Declaration of Competing Interest

Authors declare no competing financial interest exists.

Acknowledgements

Authors would like to acknowledge the support from Azerbaijan Medical University.

References

Bento, A.P., Gaulton, A., Hersey, A., Bellis, L.J., Chambers, J., Davies, M., Krüger, F.A., Light, Y., Mak, L., McGlinchey, S., Nowotka, M., Papadatos, G., Santos, R., Overington, J.P., 2014. The ChEMBL bioactivity database: an update. Nucleic Acids Res. 42, D1083–D1090. https://doi.org/10.1093/nar/gkt1031.

Bieri, C., Ernst, O.P., Heyse, S., Hofmann, K.P., Vogel, H., 1999. Micropatterned immobilization of a G protein–coupled receptor and direct detection of G protein activation. Nat. Biotechnol. 17, 1105–1108. https://doi.org/10.1038/15090.

Blake, A.D., Bot, G., Freeman, J.C., Reisine, T., 1997. Differential opioid agonist regulation of the mouse mu opioid receptor. J. Biol. Chem. 272, 782–790.

Copeland, R.A., Pompliano, D.L., Meek, T.D., 2006. Drug–target residence time and its implications for lead optimization. Nat. Rev. Drug Discov. 5, 730–739.

Deganutti, G., Zhukov, A., Deflorian, F., Federico, S., Spalluto, G., Cooke, R.M., Moro, S., Mason, J.S., Bortolato, A., 2017. Impact of protein–ligand solvation and desolvation on transition state thermodynamic properties of adenosine A2A ligand binding kinetics. Silico Pharmacol. https://doi.org/10.1007/s40203-017-0037-x.

Fábián, G., Benyhe, S., Farkas, J., Szücs, M., 1996. Thermodynamic parameters of opioid binding in the presence and absence of G-protein coupling. J. Recept. Signal Transduct. 16, 151–168. https://doi.org/10.3109/10799899609039946.

Grisshammer, R., Duckworth, R., Henderson, R., 1993. Expression of a rat neurotensin receptor in Escherichia coli. Biochem. J. 295 (Pt 2), 571–576. https://doi.org/10.1042/BJ2950571.

Grissinger, M., 2011. Keeping patients safe from methadone overdoses. Pharm. Ther. 36, 462.

Huestis, M.A., Cone, E.J., Pirnay, S.O., Umbricht, A., Preston, K.L., 2013. Intravenous buprenorphine and norbuprenorphine pharmacokinetics in humans. Drug Alcohol Depend. 131, 258–262. https://doi.org/10.1016/j.drugalcdep.2012.11.014.

Husbands, S.M., Breeden, S.W., Grivas, K., Lewis, J.W., 1999. Ring constrained analogues of the orvinols: the furanomorphides. Bioorg. Med. Chem. Lett. 9, 831–834. https://doi.org/10.1016/S0960-894X(99)00085-2.

Jamison, R.N., Raymond, S.A., Slawsby, E.A., Nedeljkovic, S.S., Katz, N.P., 1998. Opioid therapy for chronic noncancer back pain. A randomized prospective study. Spine (Phila Pa 1976) 23, 2591–2600.

Jastrzebska, B., Debinski, A., Filipek, S., Palczewski, K., 2011. Role of membrane integrity on G protein-coupled receptors: rhodopsin stability and function. Prog. Lipid Res. 50, 267–277. https://doi.org/10.1016/j.plipres.2011.03.002.

Karlsson, O.P., Löfås, S., 2002. Flow-mediated on-surface reconstitution of G-protein coupled receptors for applications in surface plasmon resonance biosensors. Anal. Biochem. 300, 132–138. https://doi.org/10.1006/abio.2001.5428.

Katz, N., 2005. Methodological issues in clinical trials of opioids for chronic pain. Neurology 65, S32–S49. https://doi.org/10.1212/WNL.65.12_SUPPL_4.S32.

Kilpatrick, G.J., Smith, T.W., 2005. Morphine-6-glucuronide: actions and mechanisms. Med. Res. Rev. 25, 521–544. https://doi.org/10.1002/med.20035.

Krantz, M.J., Garcia, J.A., Mehler, P.S., 2005. Effects of buprenorphine on cardiac repolarization in a patient with methadone-related torsade de pointes. Pharmacotherapy 25, 611–614. https://doi.org/10.1592/phco.25.4.611.61020.

Lalovic, B., Kharasch, E., Hoffer, C., Risler, L., Liuchen, L., Shen, D., 2006. Pharmacokinetics and pharmacodynamics of oral oxycodone in healthy human subjects: role of circulating active metabolites. Clin. Pharmacol. Ther. 79, 461–479. https://doi.org/10.1016/j.clpt.2006.01.009.

Li, J.-G., Raffa, R.B., Cheung, P., Tzeng, T.-B., Liu-Chen, L.-Y., 1998. Apparent thermodynamic parameters of ligand binding to the cloned rat μ-opioid receptor. Eur. J. Pharmacol. 354, 227–237. https://doi.org/10.1016/S0014-2999(98)00444-0.

Ma, Y., Kubicek, J., Labahn, J., 2013. Expression and purification of functional human mu opioid receptor from E. coli. PLoS One 8, e56500. https://doi.org/https://doi.org/10.1371/journal.pone.0056500.

Mercadante, S., Casuccio, A., Agnello, A., Serretta, R., Calderone, L., Barresi, L., 1998. Morphine versus methadone in the pain treatment of advanced-cancer patients followed up at home. J. Clin. Oncol. 16, 3656–3661. https://doi.org/10.1200/JCO.1998.16.11.3656.

Micsonai, A., Wien, F., Kernya, L., Lee, Y.-H., Goto, Y., Réfrégiers, M., Kardos, J., 2015. Accurate secondary structure prediction and fold recognition for circular dichroism spectroscopy. Proc. Natl. Acad. Sci. 112, E3095–E3103. https://doi.org/10.1073/pnas.1500851112.

Muller, I., Sarramégna, V., Milon, A., Talmont, F.J., 2010. The N-terminal end truncated mu-opioid receptor: from expression to circular dichroism analysis. Appl. Biochem. Biotechnol. 160, 2175–2186. https://doi.org/10.1007/s12010-009-8715-8.

Nikolaev, V.O., Boettcher, C., Dees, C., Bü Nemann, M., Lohse, M.J., Zenk, M.H., 2007. Live cell monitoring of-opioid receptor-mediated G-protein activation reveals strong biological activity of close morphine biosynthetic precursors. J. Biol. Chem. 282, 27126–27132. https://doi.org/10.1074/jbc.M703272200.

O'Shannessy, D.J., Brigham-Burke, M., Soneson, K.K., Hensley, P., Brooks, I., 1993. Determination of rate and equilibrium binding constants for macromolecular interactions using surface plasmon resonance: use of nonlinear least squares analysis methods. Anal. Biochem. 212, 457–468.

Pellissier, L.P., Gandía, J., Laboute, T., Becker, J.A.J., Le Merrer, J., 2017. μ opioid receptor, social behaviour and autism spectrum disorder: reward matters. Br. J. Pharmacol. https://doi.org/10.1111/bph.13808.

Petrone, D., Kamin, M., Olson, W., 1999. Slowing the titration rate of tramadol HCl reduces the incidence of discontinuation due to nausea and/or vomiting: a double-blind randomized trial. J. Clin. Pharm. Ther. 24, 115–123. https://doi.org/10.1046/j.1365-2710.1999.00203.x.

Ren, H., Yu, D., Ge, B., Cook, B., Xu, Z., Zhang, S., 2009. High-level production, solubilization and purification of synthetic human GPCR chemokine receptors CCR5, CCR3, CXCR4 and CX3CR1. PLoS One 4, e4509. https://doi.org/10.1371/journal.pone.0004509.

Rich, R.L., Myszka, D.G., 2000. Advances in surface plasmon resonance biosensor analysis. Curr. Opin. Biotechnol. 11, 54–61. https://doi.org/10.1016/S0958-1669(99)00054-3.

Rich, R.L., Errey, J., Marshall, F., Myszka, D.G., 2011. Biacore analysis with stabilized G-protein-coupled receptors. Anal. Biochem. 409, 267–272. https://doi.org/10.1016/J.AB.2010.10.008.

Savitzky, A., Golay, M.J.E., 1964. Smoothing and differentiation of data by simplified least squares procedures. Anal. Chem. 36, 1627–1639. https://doi.org/10.1021/ac60214a047.

Schlechtingen, G., DeHaven, R.N., Daubert, J.D., Cassel, J.A., Chung, N.N., Schiller, P.W., Taulane, J.P., Goodman, M., 2003. Structure-activity relationships of dynorphin a analogues modified in the address sequence. J. Med. Chem. 46, 2104–2109. https://doi.org/10.1021/jm020125+.

Sharma, G., First, E.A., 2009. Thermodynamic analysis reveals a temperature-dependent change in the catalytic mechanism of bacillus stearothermophilus tyrosyl-tRNA synthetase. J. Biol. Chem. 284, 4179–4190. https://doi.org/10.1074/jbc.M808500200.

Stanasila, L., Massotte, D., Kieffer, B.L., Pattus, F., 1999. Expression of δ, κ and μ human opioid receptors in Escherichia coli and reconstitution of the high-affinity state for agonist with heterotrimeric G proteins. Eur. J. Biochem. 260, 430–438. https://doi.org/10.1046/j.1432-1327.1999.00187.x.

Stenlund, P., Babcock, G.J., Sodroski, J., Myszka, D.G., 2003. Capture and reconstitution of G protein-coupled receptors on a biosensor surface. Anal. Biochem. 316, 243–250. https://doi.org/10.1016/S0003-2697(03)00046-0.

Strange, P.G., 2010. Use of the GTPγS ([35S]GTPγS and Eu-GTPγS) binding assay for analysis of ligand potency and efficacy at G protein-coupled receptors. Br. J. Pharmacol. 161, 1238–1249. https://doi.org/10.1111/j.1476-5381.2010.00963.x.

Swinney, D., 2006. Can binding kinetics translate to a clinically differentiated drug? From theory to practice. Lett. Drug Des. Discov. 3, 569–574.

Tucker, J., Grisshammer, R., 1996. Purification of a rat neurotensin receptor expressed in Escherichia coli. Biochem. J. 317 (Pt 3), 891–899. https://doi.org/10.1042/BJ3170891.

Vögler, O., Barceló, J.M., Ribas, C., Escribá, P.V., 2008. Membrane interactions of G proteins and other related proteins. Biochim. Biophys. Acta Biomembr. 1778, 1640–1652. https://doi.org/10.1016/J.BBAMEM.2008.03.008.

de Witte, W.E.A., Danhof, M., van der Graaf, P.H., de Lange, E.C.M., 2016. In vivo target residence time and kinetic selectivity: the association rate constant as determinant. Trends Pharmacol. Sci. 37, 831–842. https://doi.org/10.1016/J.TIPS.2016.06.008.

Yassen, A., Olofsen, E., van Dorp, E., Sarton, E., Teppema, L., Danhof, M., Dahan, A., 2007. Mechanism-based pharmacokinetic-pharmacodynamic modelling of the reversal of buprenorphine-induced respiratory depression by naloxone. Clin. Pharmacokinet. 46, 965–980. https://doi.org/10.2165/00003088-200746110-00004.

Zhang, Z., Melia, T.J., He, F., Yuan, C., McGough, A., Schmid, M.F., Wensel, T.G., 2004. How a G protein binds a membrane. J. Biol. Chem. 279, 33937–33945. https://doi.org/10.1074/JBC.M403404200.